Semiconductor Physics, Quantum Electronics & Optoelectronics, 2023. V. 26, No 2. P. 208-214.

Optics

The spectral and microscopical study of phytosynthesized plasmonic gold nanoparticles

V. Bartošová[1], R. Smolková[1], L.M. Grishchenko[2], R.P. Linnik[3], V.V. Lisnyak[3], R. Mariychuk[1*]

[1]*University of Prešov, Faculty of Humanity and Natural Sciences, Department of Ecology, 17th November 1, Prešov 08116, Slovakia*
[2]*Taras Shevchenko National University of Kyiv, Faculty of Radiophysics, Electronics and Computer Systems, 4g, Glushkova ave., 03127 Kyiv, Ukraine*
[3]*Taras Shevchenko National University of Kyiv, Chemical Faculty, 64/13, Volodymyrska str., 01601 Kyiv, Ukraine*
[*]*Corresponding author e-mail: ruslan.mariychuk@unipo.sk*

Abstract. Here, we present a facile and environmentally friendly method for the synthesis of gold nanoparticles (Au NPs) with an infrared response. The structure of the obtained Au NPs was investigated by transmission electron microscopy. Small and large Au NPs with different morphologies, including spheres, triangles, and hexagons, were imaged and studied, and the reasons for the morphological diversity were discussed. From the selected area diffraction data, the Au NPs showed sufficient crystallinity. The optical properties of the Au nanocolloids, investigated by UV-visible absorption spectroscopy, confirmed the presence of localized surface plasmon resonance (LSPR) peaks at 500…540 nm for Au NPs smaller than 30 nm. An increase in absorption intensity in the 600…1050 nm region indicates the formation of larger non-spherical Au NPs. The optical absorption spectra show the redshift of the second LSPR peak to the near-infrared region with a longer wavelength with increasing $HAuCl_4$ concentration in the synthesis solution. In addition, we recorded the maxima of photoluminescence (PL) bands at 370 and 458 nm for the water-diluted Au colloids under 320 nm excitation and considered the possible reasons for PL. Attempts were made to elucidate the optical and PL behavior of the nanocolloids within the known models.

Keywords: optical absorbance, surface plasmon resonance, photoluminescence, gold nanoparticles.

https://doi.org/10.15407/spqeo26.02.208
PACS 68.37.Lp, 73.20.Mf, 78.40.-q, 78.67.Bf, 78.67.-n

Manuscript received 03.05.23; revised version received 18.05.23; accepted for publication 07.06.23; published online 26.06.23.

1. Introduction

Nanotechnology is a new and exciting field of modern materials science that deals with nanoscale objects of various materials with sizes of 10^{-9}…10^{-7} m [1–3]. Nanoparticles (NPs) of noble metals, such as gold, silver, platinum, *etc*., have attracted considerable interest in recent years due to their unique electrical, magnetic, catalytic, and optical properties. Gold nanoparticles (Au NPs) are among the most prominent metal NPs that have been extensively used in various fields [4, 5] due to their high reactivity, stability, surface functionalization, low toxicity, and strong absorption of visible light by surface plasmon resonance (SPR). For example, they can be used as advanced sensors in photothermal therapy and in controlled drug release systems [6–8]. The synthesis of Au NPs can be performed by chemical, physical, and "green synthesis" methods [9–11]. Physical methods usually do not involve toxic chemicals. But they require expensive equipment with limited control over the morphology of the resulting NPs. This disadvantage can be overcome by the use of chemical methods. However, the most reliable protocols usually involve the use and release of harmful and toxic chemical compounds [12–15]. This limits not only the synthesis process but also the application of the resulting nanoparticles in biological systems (*e.g*., nanomedicine). Therefore, they are slowly being replaced by so-called green synthesis methods, which consist in using renewable natural materials that are easily accessible, cheap, safe, and environmentally friendly. At the same time, the resulting metal NPs remain biocompatible, which is one of the key requirements for their use in nanomedicine. The use of phytochemicals for production, also called phytosynthesis, offers a wide range of possibilities due to the diversity of plants. However, despite the above advantages, the

synthesis of metal NPs from biological systems is very complex. In particular, the study and understanding of the NP formation processes are necessary for the development of products with controlled morphology (size and shape). The optical properties of Au NPs depend on the size, but more importantly on the shape. While spherical Au NPs exhibit the SPR absorption maximum at 530…560 nm (depending on the size), non-spherical Au NPs absorb the radiation in the near-infrared region (> 650 nm) [16]. This makes them promising for nanomedicine applications due to the strong light absorption within the biological transparency window of 650…1350 nm [17, 18].

Therefore, this study focuses on the synthesis and characterization of biocompatible Au NPs prepared using extracts of medicinal plants (peppermint) with responses in the infrared region.

2. Experimental

2.1. Preparation of plant extract and synthesis of Au nanoparticles

An aqueous extract of peppermint (*M. piperita*, cv. 'Perpeta') was prepared by maceration of well-grained dry leaves collected from the Botanical Garden of the University of Prešov (Prešov, Slovak Republic) in hot double-distilled water 1:10 (weight to volume) for 30 min at 100 °C. The obtained extract was first filtered through KA 1-M filter paper (Papírna Pernštejns. s.r.o., Czech Republic) and then centrifuged on a micro-processor-controlled centrifuge (Centronic BL-II, J.P. Selecta) at 3000 min^{-1} for 30 min to remove small plant particles. The dry matter content of the aqueous extract obtained was determined using a Shimadzu MOC-120H moisture analyzer. The obtained extract was divided into 2 ml Eppendorf tubes and frozen at –18 °C until used in the synthesis experiments.

Nanocolloid solutions of Au NPs were prepared at room temperature (23 °C) by direct interaction of 1 mM $HAuCl_4$ (Thermoscientific, 99.99% metal basis) aqueous solution with aqueous plant extract under continuous mixing. The concentration of Au^{3+} was adjusted by varying the volumes of extract and double-distilled water. The stable nanocolloidal Au NPs solutions were obtained for the extract concentration from 0.125 to 1 mg/ml and Au^{3+} in the range of 0.025 to 0.975 mmol [19].

The LSPR of Au NPs was evaluated by examining the UV-Vis absorbance of each NP colloidal solution. Absorption spectra were recorded in the spectral range of 190…1400 nm with a 1 nm scan step using a Shimadzu UV-2600 UV-Vis spectrophotometer equipped with the photomultiplier and InGaAs semiconductor detectors, and the UV Probe 2.42 software. The position and profile of the LSPR band provide information on NP dispersion and allow the average NP size to be estimated. Spectra were processed using SpectraGryph 1.2 spectroscopy software [20] and fitted using Fityk [21]. Photoluminescence excitation and emission spectra were recorded using a Perkin-Elemer LS-55 fluorescence/luminescence spectrophotometer with a pulsed high-pressure xenon source.

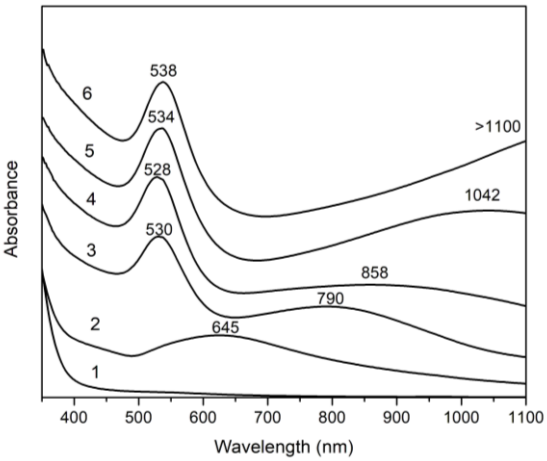

Fig. 1. UV-Vis spectra of *Mentha piperita* mediated Au NPs prepared with different concentrations of Au^{3+} (*1* – 0.0250, *2* – 0.2500, *3* – 0.3750, *4* – 0.5000, *5* – 0.5625, *6* – 0.7500 mM).

Structural studies and particle size estimates were performed by transmission electron microscopy (TEM) using high-resolution TEM images taken on a JEOL JEM-2010 instrument with an accelerating voltage of 200 kV (JEOL Ltd., Tokyo, Japan). The TEM image was captured with a GatanUltraScan 1000 digital camera in 2048×2048 pixels in 16 bits over an area of approximately 0.8×0.8 inch on the large phosphor screen. Samples were prepared by dropping 10 μL of a colloidal Au NP solution onto a perforated carbon-coated Cu grid and drying for 6 h. The TEM images were acquired in bright field (BF) and were analyzed using the Fiji software from ImageJ [22]. A GIF Tridiem post-column energy filter on the JEOL JEM 2100 F instrument was used for the acquisition of energy-filtered images and selected area electron diffraction (SAED) studies [23].

3. Results and discussion

3.1. Structural and optical properties

Nanocolloid solutions containing *M. piperita*-mediated Au NPs were obtained in a range of extract concentrations from 0.125 to 1.0 mg/ml, with the initial concentration of Au^{3+} in the range of 0.025 to 0.9750 mmol. The presence of biosynthesized Au NPs in the nanocolloids was confirmed by the colorimetric method since the color of the reaction solution changed to dark red after mixing the plant extract with $HAuCl_4$. Fig. 1 shows representative spectra of the obtained colloids for selected samples with the extract concentration of 0.25 mg/ml. One can clearly see the presence of two localized surface plasmon resonance (LSPR) absorption maxima that are influenced by the concentration of Au^{3+} in the reaction mixture. The first, at the wavelength of 528…538 nm, is typical for spherical Au NPs. The second, in the near infrared (NIR) region, indicates the presence of non-spherical Au NPs. Since the position of this maximum is very sensitive to size and aspect ratio, the broadening and bathochromic shift of the second LSPR peak increase with increasing Au^{3+} concentration.

For samples with Au^{3+} concentrations of 0 to 0.6 mmol, the position of the LSPR peak can be monitored with a standard photometer; at higher concentrations, the peak position crosses the value of 1100 nm.

In general, the position of the maximum and the width of the LSPR bands can also indicate a change in the degree of homogeneity of Au NPs. The spectra show a variation of the maximum of the LSPR peak around 528…538 nm, which shifts to the NIR region with time and the concentration of Au^{3+} ions in solution. The peak around 528 nm clearly indicates the presence of small Au NPs presumably spherical and triangular NPs. Typically, LSPR arises as a collective coherent oscillation of conduction electrons relative to a positive metallic lattice when small metallic NPs are excited by the electromagnetic field of incident light [24]. According to literature data [11, 14, 15], the LSPR band of spherical Au NPs is located around 500…540 nm for Au NPs smaller than 30 nm. No significant differences in the position of the main absorption peak were found for a number of recorded spectra of Au NPs colloids. The broad shoulder above 650 nm, together with a general increase in absorption intensity in the 600…1050 nm region, indicates the formation of larger and non-spherical Au NPs.

The broad LSPR band profile may be a consequence of the higher size dispersion of small Au NPs. The large number of surface atoms in small Au NPs increases the attenuation of electron oscillations in the conduction band, which can be realized due to the loss of iteration of electrons involved in surface bonding. We have used a method to estimate the size of Au NPs from absorption spectra that is valid for plasmonic Au NPs smaller than 30 nm. This empirical model for NP size estimation from UV-Vis spectra takes into account the LSPR absorbance relative to the typical Au absorbance at 450 nm. This is because an empirical relationship has been established between the logarithm of the NP size and the ratio of the absorbance intensities at the maxima of the LSPR absorption peak (A_{LSPR}) and the absorbance at 450 nm (A_{450}). The following expression was used for the estimation by the Haiss method [25]:

$$d = \exp\left(B_1 \frac{A_{LSPR}}{A_{450}} - B_2 \right), \quad (1)$$

where B_1 = 3.55 and B_2 = 3.11 are the inverse of the slope and the intercept, respectively, obtained from the linear fit of the plot of the logarithm of the Au NP size *versus* the A_{SPR}/A_{450} ratio. However, these estimated dimensions assigned to Au nanospheres showed growth in the range of 3.0 to 6.5 nm with increasing $C(HAuCl_4)$ concentration from 0.025 to 0.56 mmol. At higher concentrations, we observed the reverse dependence and the size of Au nanospheres decreased in the range of 5.8 to 3.1 nm with increasing $C(HAuCl_4)$ concentration from 0.625 to 0.975 mmol.

High absorption cross sections in the visible and infrared regions make small metallic NPs promising agents for bioimaging and hyperthermia treatment.

Typically, the maximum position of the LSPR band is affected by the size, shape, interparticle distance, and dielectric constant and refractive index of the medium; all these parameters can shift the LSPR, *e.g.*, into the NIR region [26–29]. According to the Lambert–Beer law, the absorbance is directly proportional to the extinction coefficient multiplied by the path length and the concentration of the solution. Therefore, a lower absorbance in the spectra indicates a low concentration of Au NPs. According to Mie's theory, the vibrational modes depend on the size of the particles, and as the size decreases, the maximum absorbance decreases and blue shifts. The absorption is expected to increase as the size of Au NPs increases because the mean free path of electrons also increases.

Fig. 2 shows the shape and size of the resulting Au NPs using the TEM technique after synthesis. The rapid reduction of Au ions by the aqueous extract of *Mentha piperita* allowed the homogeneous nucleation of gold metals, resulting in the formation of Au NPs of small size. Au NPs are confined within a *Mentha piperita* medium composed of biomolecules that act as stabilizers and capping agents during synthesis. The resulting Au NPs were found to contain spherical Au NPs in the size range of 6.5 to 15 nm (Fig. 2a). In rare cases, the spherical Au NPs with larger sizes were also observed in the sample, but their number was rather small (Fig. 2e).

The lower magnification TEM images (Fig. 2b to d) show that the Au NPs are spheres, triangles to hexagons. In addition, large Au NPs can be crystallized from a concentrated solution of $HAuCl_4$ (Fig. 2e). The SAED pattern of such face-centered (fcc) crystallized NPs (Fig. 2e) shows dots superimposed on rings. This pattern may show the polycrystalline structure composed of multiple sub-crystals and/or contain partially amorphous structures (Fig. 2e). The prepared Au nanoplates typically have larger sizes with diagonal lengths of 100 ± 5 nm. In the prepared nanocolloids, the ratio of Au triangles to hexagons, both with diagonal lengths of 20 to 42 nm, is strongly dependent on stacking defects. These types of defects are common in densely packed lattices. For fcc cubic Au with twin planes or stacking planar defects, hexagonal Au plates form at very early stages of growth. They form due to the sixfold symmetry of the fcc gold lattice. The presence of planar defects in Au NPs is one reason why the six-sided faces, in this case, the ends of the defect plane, can form alternating concave and convex surfaces that regulate the addition of Au atoms. For triangular seeds, in a crystal with a single planar defect, the rapid addition of Au to the concave sides causes them to grow to some extent, resulting in a triangular Au plate whose side faces are bounded by three convex sides. This configuration is not conducive to atomic addition.

The PL emission spectra of the concentrated solution of the as-prepared Au colloids by excitation at 240 and 320 nm gave a negligible emission, so, the colloid solutions were diluted 2 and 16 times for future studies.

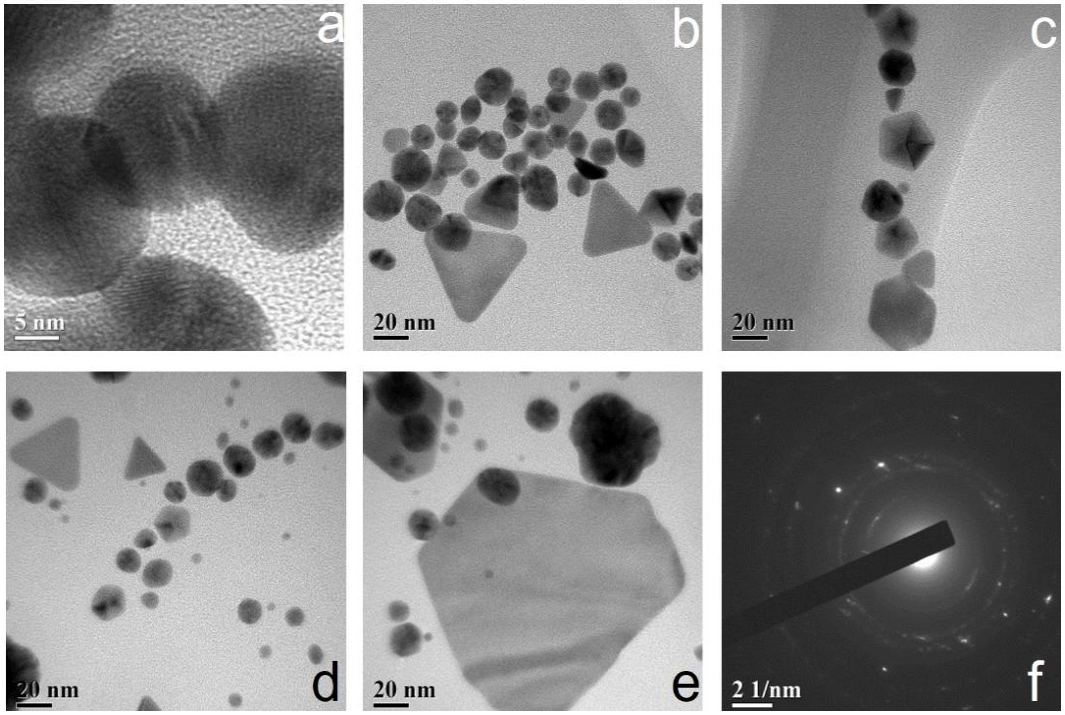

Fig. 2. Higher magnification TEM BF image of (a) Au spheres and TEM BF images of Au NPs: (b) triangles, (c) hexagons and triangles, (d) spheres, hexagons, and triangles, (e) pseudospheres and large hexagons, (f) SEAD pattern, here the strongest spots could be assigned to the {220} reflections.

The maxima of the PL emission spectra ($\lambda_{em}^{\max} = 370$ nm and 458 nm , $\lambda_{ex}^{\max} = 320$ nm) and their shape indicate the presence of aggregates in the solution (Fig. 3). To this day, a large number of highly luminescent Au NPs with sizes ranging from 0.3 to 20 nm have been synthesized [30]. Two important papers proposed a luminescence mechanism in Au NPs: interband radiative electron recombination and intraband (sp–sp) and interband (sp–d) transitions occur in small molecular Au nanoclusters (Au NCs) [30, 31]. Chen and co-authors [32] reported tunable emission from UV to NIR in Au NPs. The emission of these Au NPs is usually attributed to the interband transition Au $5d^{10}$ to 6sp and also to the capping ligand-metal charge transfer transition [32, 33]. According to Liu and co-authors [33], there is an influence of Au NP size and surface area on the PL emission.

From a free electron gas model, the number of gold atoms *N* in small Au NCs can be calculated from the PL band position with an empirical equation

$$N_{\mathrm{Au}} = \left(\frac{e \lambda_{\max} E_{\mathrm{F}}}{hC} \right)^3, \qquad (2)$$

where *e* is a number equal to the electron charge, $\lambda_{\max}$ is a wavelength at the maximum of the emission band, E_{F} is the Fermi energy of bulk gold (5.53 eV), *h* is the Planck constant, and *c* is the speed of light. According to the equation, NPs exhibiting PL peaks in the shorter wavelength region mentioned above are small and consist of about 9 to 6 Au atoms, which is in contradiction with the TEM observations. It should be noted that the emission band intensity is low for the prepared Au NPs. As we can mention, the origin of photoluminescence in Au NPs is still not clear, so the emission band can be attributed to the $5d^{10}$ to 6sp interband transition and also to the capping effect at the ligand-to-metal charge transfer transition. We have previously reported that if the PL in the Au nanocolloids is due to the transitions in the metal core [34], the emission wavelength can be tuned by increasing the NP size due to the quantum confinement effect, as proposed by Chen *et al*. [32]. In our study, the samples of Au NPs have the same capping ligands.

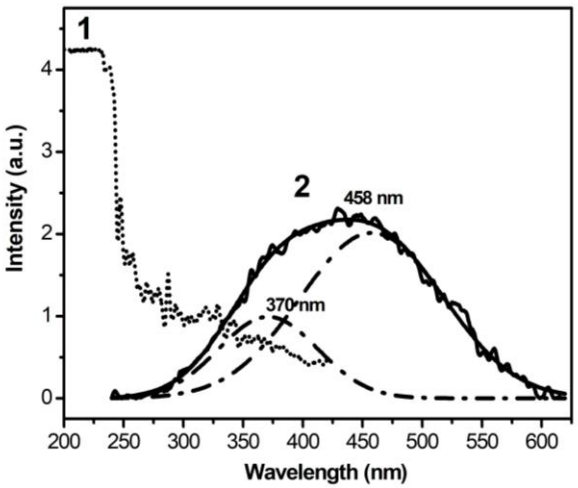

Fig. 3. Excitation spectrum (*1*) and PL spectrum (*2*) of the biosynthesized Au NPs.

Functionalization of the Au NP surface with species containing bioactive end groups, such as amino or carboxylic groups, allows subsequent coupling with relevant biomolecules. For biomedical applications, green and at-synthesis surface functionalization is a common strategy. This approach not only promotes subsequent cross-linking between Au NPs and specific biological species but also minimizes their cytotoxicity and prevents non-specific binding.

Therefore, we conclude that only the average size is the only difference between them. However, there is no clear relationship between the size and the emission wavelength. Furthermore, it can be assumed that the PL emission in these Au NPs is not mainly determined by the metal-core transitions, suggesting the influence of the capping-core transitions. The noisy profiles of the emission band suggest the presence of surface processes contributing to the emission. The surface acid synthesis may lead to non-radiative processes that reduce the enhancement of the PL emission of these Au NPs, despite the influence of the strong donor ligand. All these considerations suggest a strong surface influence on the PL behavior, which can be mainly determined by ligand-to-metal transfer transitions and surface processes.

4. Conclusions

We have prepared highly stable Au NPs functionalized with phytosynthesis products. Although Au NPs prepared by the phytosynthesis route, they exhibited the expected size homogeneity but showed a wide range of sizes and morphologies, including triangles and hexagons. TEM studies revealed a semi-homogeneous size distribution for small spherical Au NPs. The prepared Au NPs exhibited high colloidal stability at near neutral and slightly acidic pH. These colloidal solutions before dilution have poor PL emission of Au NPs. The results showed that a distinct absorption peak at about 530 nm was identified in the UV-Vis spectra, which was attributed to the LSPR induced by spherical Au NPs. These results provide new information for a possible understanding of the PL and LSPR processes, especially for complex mixtures of Au NPs, which will benefit potential applications such as optical imaging and sensing. The optical and plasmonic properties of Au NPs in aqueous colloids have been investigated. The focus of the study is on the pseudospheres, triangles, and hexagons of Au NPs determined by the TEM-SAED method. The absorption maximum is related to the LSPR of Au NPs according to the Mie theory. The UV-Vis spectra of the obtained Au NPs showed the strong SPR response in the infrared region, which makes them promising for application in nanomedicine, such as photothermal therapy.

Acknowledgements

This work was supported by the Scientific Grant Agency of the Ministry of Education, Science, Research and Sport of the Slovak Republic and the Slovak Academy of Sciences, No. 1/0882/21.

References

1. Singh A., Imtiyaz A. Applications of nano-technology in agriculture and food science: A review. *Asian J. Chem*. 2023. **35**, No 5. P. 1049–1062. https://doi.org/10.14233/ajchem.2023.27735.
2. Ramesh M., Janani R., Deepa C., Rajeshkumar L. Nanotechnology–enabled biosensors: A review of fundamentals, design principles, materials, and applications. *Biosensors*. 2023. **13**, No 1. P. 40. https://doi.org/10.3390/bios13010040.
3. Khan Y., Sadia H., Shah S.Z.A. *et al*. Classification, synthetic, and characterization approaches to nanoparticles, and their applications in various fields of nanotechnology: A review. *Catalysts*. 2022. **12**, No 11. P. 1386. https://doi.org/10.3390/catal12111386.
4. Deepa K., Sridhar A., Panda T. Biogenic gold nano-particles: Current applications and future prospects. *J. Clust. Sci*. 2023. **34**, No 3. P. 1163–1183. https://doi.org/10.1007/s10876–022–02304–8.
5. Patil T., Gambhir R., Vibhute A., Tiwari A.P. Gold nanoparticles: Synthesis methods, functionalization and biological applications. *J. Clust. Sci*. 2023. **3**, No 2. P. 705–725. https://doi.org/10.1007/s10876-022-02287-6.
6. Kumar L., Verma S., Utreja P., Kumar D. Overview of inorganic nanoparticles: An expanding horizon in tumor therapeutics. *Recent Patents Anti-Canc. Drug Discov*. 2023. **18**, No 3. P. 343–363. https://doi.org/10.2174/1574892817666221005094423.
7. Barabadi H., Mobaraki K., Ashouri F. *et al*. Nano-biotechnological approaches in antinociceptive therapy: Animal-based evidence for analgesic nano-therapeutics of bioengineered silver and gold nano-materials. *Adv. Colloid Interface Sci*. 2023. **316**. P. 102917. https://doi.org/10.1016/j.cis.2023.102917.
8. Gulia K., James A., Pandey S., Dev K., Kumar D., Sourirajan A. Bio-inspired smart nanoparticles in enhanced cancer theranostics and targeted drug delivery. *J. Funct. Biomater*. 2022. **13**, No 4. P. 207. https://doi.org/10.3390/jfb13040207.
9. Jiang Z., Li L., Huang H. *et al*. Progress in laser ablation and biological synthesis processes: "Top–down" and "Bottom–up" approaches for the green synthesis of Au/Ag nanoparticles. *Int. J. Mol. Sci*. 2022. **23**, No 23. P. 14658. https://doi.org/10.3390/ijms232314658.
10. Datta D., Deepak K.S., Das B. Progress in the synthesis, characterisation, property enhancement techniques and application of gold nanoparticles: A review. *MRS Commun*. 2022. **12**, No 5. P. 700–715. https://doi.org/10.1557/s43579-022-00216-2.
11. Shah M.M., Ahmad K., Ahmad B. *et al*. Recent trends in green synthesis of silver, gold, and zinc oxide nanoparticles and their application in nanosciences and toxicity: a review. *Nanotechnol. Environ. Eng*. 2022. **7**, No 4. P. 907–922. https://doi.org/10.1007/s41204-022-00287-5.

12. Vijayaram S., Razafindralambo H., Sun Y.-Z. *et al*. Applications of green synthesized metal nanoparticles – a review. *Biol. Trace Elem. Res*. 2023. https://doi.org/10.1007/s12011-023-03645-9.
13. Roszczenko P., Szewczyk O.K., Czarnomysy R. *et al*. Biosynthesized gold, silver, palladium, platinum, copper, and other transition metal nanoparticles. *Pharmaceutics*. 2022. **14**, No 11. P. 2286. https://doi.org/10.3390/pharmaceutics14112286.
14. Verma A.K., Kumar P. On recent developments in biosynthesis and application of Au and Ag nanoparticles from biological systems. *J. Nanotechnol*. 2022. **2022**, No 2. P. 5560244. https://doi.org/10.1155/2022/5560244.
15. Mariychuk R., Grulova D., Grishchenko L.M. *et al.* Green synthesis of non-spherical gold nanoparticles using *Solidago canadensis* L. extract. *Appl. Nanosci*. 2020. **10**, No 12. P. 4817–4826. https://doi.org/10.1007/s13204-020-01406-x.
16. Mariychuk R., Porubská J., Ostafin M. *et al.* Green synthesis of stable nanocolloids of monodisperse silver and gold nanoparticles using natural polyphenols from fruits of *Sambucus nigra* L. *Appl. Nanosci*. 2022. **10**, No 12. P. 4545–4558. https://doi.org/10.1007/s13204-020-01324-y.
17. Nejabat M., Samie A., Ramezani M. *et al.* An overview on gold nanorods as versatile nanoparticles in cancer therapy. *Journal of Controlled Release*. 2023. **354**. P. 221–242. https://doi.org/10.1016/j.jconrel.2023.01.009.
18. Pratap D., Shah R.K., Khandekar S., Soni S. Photothermal effects in small gold nanorod aggregates for therapeutic applications. *Appl. Nanosci*. 2022. **12**, No 7. P. 2045–2058. https://doi.org/10.1007/s13204-022-02456-z.
19. Mariychuk R., Smolková R., Bartošová V. *et al*. The regularities of the *Mentha piperita* L. extract mediated synthesis of gold nanoparticles with a response in the infrared range. *Appl. Nanosci*. 2022. **12**, No 4. P. 1071–1083. https://doi.org/10.1007/s13204-021-01740-8.
20. Wojdyr M. *Fityk*: A general–purpose peak fitting program. *J. Appl. Cryst*. 2010. **43**, No 1. P. 1126–1128. https://doi.org/10.1107/S0021889810030499.
21. Menges F. Spectragryph Optical Spectroscopy Software, Version 1.2.14. Available online: http://www.effemm2.de/spectragryph/ (accessed on 22 July 2020).
22. Schindelin J., Arganda-Carreras I., Frise E. *et al*. Fiji: an open-source platform for biological-image analysis. *Nature Methods*. 2012. **9**, No 7. P. 676–682. https://doi.org/10.1038/nmeth.2019.
23. Tsapyuk G.G., Diyuk V.E., Mariychuk R. *et al*. Effect of ultrasonic treatment on the thermal oxidation of detonation nanodiamonds. *Appl. Nanosci*. 2020. **10**, No 12. P. 4991–5001. https://doi.org/10.1007/s13204-020-01277-2.
24. Hutter E., Fendler J.H. Exploitation of localized surface plasmon resonance. *Adv. Mater*. 2004. **16**, No 19. P. 1685–1706. https://doi.org/10.1002/adma.200400271.
25. Haiss W., Thanh N.T.K., Aveyard J., Fernig D.G. Determination of size and concentration of gold nanoparticles from UV–vis spectra. *Analyt. Chem*. 2007. **79**, No 11. P. 4215–4221. https://doi.org/10.1021/ac0702084.
26. Haes A.J., Zou S.L., Schatz G.C., Van Duyne R.P. A nanoscale optical biosensor: The long range distance dependence of the localized surface plasmon resonance of noble metal nanoparticles. *J. Phys. Chem. B*. 2004. **108**, No 1. P. 109–116. https://doi.org/10.1021/jp0361327.
27. Hegde H.R., Chidangil S., Sinha R.K. Refractive index sensitivity of Au nanostructures in solution and on the substrate. *J. Mater. Sci.: Mater. Electron*. 2022. **33**, No 7. P. 4011–4024. https://doi.org/10.1007/s10854-021-07593-9.
28. Sui M., Kunwar S., Pandey P. *et al*. Strongly confined localized surface plasmon resonance (LSPR) bands of Pt, AgPt, AgAuPt nanoparticles. *Sci. Rept*. 2019. **9**, No 1. P. 16582. https://doi.org/10.1038/s41598-019-53292-1.
29. Rasskazov I.L., Carney P.S., Moroz A. Intriguing branching of the maximum position of the absorption cross section in Mie theory explained. *Opt. Lett*. 2020. **45**, No 14. P. 4056–4059. https://doi.org/10.1364/OL.397782.
30. Zheng J., Zhou C., Yu M., Liu J. Different sized luminescent gold nanoparticles. *Nanoscale*. 2012. **4**. P. 4073–4083. https://doi.org/10.1039/C2NR31192E.
31. Wilcoxon J.P., Martin J.E., Parsapour F. *et al.* Photoluminescence from nanosize gold clusters. *J. Chem. Phys*. 1998. **108**, No 21. P. 9137–9143. https://doi.org/10.1063/1.476360.
32. Chen W., Tu X., Guo X. Fluorescent gold nanoparticles-based fluorescence sensor for Cu^{2+} ions. *Chem. Commun*. 2009. **7**, No 13. P. 1736–1738. https://doi.org/10.1039/b820145e.
33. Liu B., Wang Y., Deng M. *et al.* Blue light emitting gold nanoparticles functionalized with non–thiolate thermosensitive polymer ligand: Optical properties, assemblies and application. *RSC Adv*. 2014. **4**, No 100. P. 57245–57249. https://doi.org/10.1039/c4ra09335f.
34. Mariychuk R., Fejer J., Linnik R.P. *et al.* Green synthesis and photoluminescence properties of gold nanoparticles with irregular shapes. *Mol. Cryst. Liq. Cryst*. 2023. **751**, No 1. P. 48–55. https://doi.org/10.1080/15421406.2022.2073528.

Authors' contributions

Bartošová V.: investigation, visualization, writing – original draft.
Smolková R.: investigation, visualization.
Grishchenko L.M.: investigation, methodology.
Linnik R.P.: investigation, methodology.
Lisnyak V.V.: methodology, visualization, conceptualization, writing – original draft, writing – review & editing.
Mariychuk R.: methodology, writing – original draft, writing – review & editing, methodology, supervision.

Authors and CV

Viktoria Bartošová is a doctoral student at the Department of Ecology of the University of Prešov, Slovakia. Co-author of one publication indexed in Scopus and Web of Science databases. Her scientific interest is the ecological synthesis of metal nanoparticles.
E-mail: viktoria.bartosova.1@smail.unipo.sk,
https://orcid.org/0009-0000-2471-6095

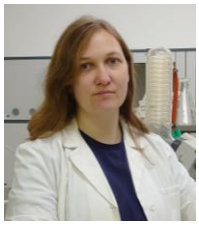

Romana Smolková, PhD, is a research associate at the Department of Ecology, University of Presov, Slovakia. Author of 16 publications indexed in Scopus and Web of Science databases. Her research interests include bioinorganic chemistry, medicinal chemistry, and sustainable synthesis of nanomaterials.
E-mail: romana.smolkova@unipo.sk,
https://orcid.org/0000-0003-2086-3906

Rostyslav P. Linnik, PhD, is an assistant professor at the Department of Analytical Chemistry, Taras Shevchenko National University of Kyiv, Ukraine. Author of about 38 publications indexed in Scopus and Web of Science databases. His research interests include analytical chemistry, kinetic (chemiluminescence), voltammetric, chromatographic methods of studying coexisting forms of elements. E-mail: rostyslavlinnik@knu.ua,
https://orcid.org/0000-0002-6401-8184

Vladyslav V. Lisnyak, DSc, is a senior researcher at the Department of Analytical Chemistry, Taras Shevchenko National University of Kyiv, Ukraine. Author of more than 150 publications indexed in Scopus and Web of Science databases and 38 patents. His research interests include analytical and physical chemistry, nanomaterials and materials science.
https://orcid.org/0000-0002-6820-1445,
e-mail: lisnyak@univ.kiev.ua, vladyslav.lisnyak@knu.ua

Liudmyla M. Grishchenko, PhD, is an assistant professor at the Department of Medical Radiophysics, Faculty of Radiophysics, Electronics and Computer Systems, Taras Shevchenko National University of Kyiv, Ukraine. Author of over 60 publications indexed in Scopus and Web of Science databases and 6 patents. Her research interests include physical chemistry, carbon nanomaterials, and physical sciences.
E-mail: ludmila_grischenko@knu.ua,
http://orcid.org/0000-0002-0342-4859

Ruslan Mariychuk, PhD, is an associate professor at the Department of Ecology, University of Presov, Slovakia. Author of over 60 publications indexed in Scopus and Web of Science databases and 3 patents. His research interests include green chemistry, sustainable synthesis of nanomaterials, and materials science.
https://orcid.org/0000-0001-8464-4142

Спектральне та мікроскопічне дослідження фітосинтезованих плазмонних наночастинок золота

V. Bartošová , R. Smolková, Л.М. Грищенко, Р.П. Лінник, В.В. Лісняк, Р. Марійчук

Анотація. У цій роботі представлено простий та екологічно чистий метод синтезу наночастинок золота (Au НЧ) з відгуком в інфрачервоній області. Методом трансмісійної електронної мікроскопії досліджено структуру отриманих Au НЧ. Менші та більші Au НЧ з різною морфологією, включаючи сфери, трикутники та шестикутники, було виявлено та вивчено, а також обговорено причини морфологічної різноманітності. Результати дифракції вибраних ділянок Au НЧ показали достатньо високу кристалічність. Оптичні властивості наноколоїдів Au, досліджені за допомогою УФ видимої абсорбційної спектроскопії, підтвердили наявність піків локалізованого поверхневого плазмонного резонансу (ЛППР) при 500…540 нм для Au НЧ розміром меншим за 30 нм. Збільшення інтенсивності поглинання в області 600…1050 нм свідчить про утворення більших несферичних Au НЧ. Спектри оптичного поглинання показують червоне зміщення другого піка ЛППР у ближню інфрачервону область із більшою довжиною хвилі зі збільшенням концентрації $HAuCl_4$ у реакційній суміші. Крім того, було зафіксовано максимуми смуг фотолюмінесценції при 370 і 458 нм для розбавлених водою колоїдів Au НЧ при збудженні 320 нм та розглянуто можливі причини фотолюмінесценції. Було зроблено спроби з'ясувати оптичну та фотолюмінесцентну поведінку наноколоїдів у рамках відомих моделей.

Ключові слова: оптичне поглинання, поверхневий плазмонний резонанс, фотолюмінесценція, наночастинки золота.